



Dissolution behavior and early bone apposition of calcium phosphate-coated machined implants

Ji-Wan Hwang^{†,‡}, Eun-Ung Lee^{†,‡}, Jung-Seok Lee[‡], Ui-Won Jung[‡], In-Seop Lee[‡], Seong-Ho Choi^{*,†}

[†]Department of Periodontology, Research Institute for Periodontal Regeneration, Yonsei University College of Dentistry, Seoul, Korea

[‡]Institute of Physics & Applied Physics, Atomic-Scale Surface Science Research Center, Yonsei University, Seoul, Korea

Purpose: Calcium phosphate (CaP)-coated implants promote osseointegration and survival rate. The aim of this study was to (1) analyze the dissolution behavior of the residual CaP particles of removed implants and (2) evaluate bone apposition of CaP-coated machined surface implants at the early healing phase.

Methods: Mandibular premolars were extracted from five dogs. After eight weeks, the implants were placed according to drilling protocols: a nonmobile implant (NI) group and rotational implant (RI) group. For CaP dissolution behavior analysis, 8 implants were removed after 0, 1, 2, and 4 weeks. The surface morphology and deposition of the coatings were observed. For bone apposition analysis, block sections were obtained after 1-, 2-, and 4-week healing periods and the specimens were analyzed.

Results: Calcium and phosphorus were detected in the implants that were removed immediately after insertion, and the other implants were composed mainly of titanium. There were no notable differences between the NI and RI groups in terms of the healing process. The bone-to-implant contact and bone density in the RI group showed a remarkable increase after 2 weeks of healing.

Conclusions: It can be speculated that the CaP coating dissolves early in the healing phase and chemically induces early bone formation regardless of the primary stability.

Keywords: Calcium phosphate, Dental implantation, Osseointegration.

INTRODUCTION

The implant surface plays an important role in enhancing osseointegration and achieving rapid secondary stability [1]. Roughening the implant surface through surface treatments may promote osteogenesis by increasing the surface area, enhancing cellular activity, and ultimately increasing bone attachment [2]. A systematic review by Shalabi et al. [3] concluded that there was a positive correlation between surface roughness and bone-to-implant contact. As a consequence, over the last 30 years, various surface modification techniques

have been introduced, including blasting, etching, oxidizing, titanium (Ti) plasma spraying, and incorporation of hydroxyapatite (HA) or other forms of calcium phosphate (CaP) [4].

CaP has been investigated extensively because of its biocompatibility and mineral chemistry, which resembles that of human bone [5]. Moreover, as a coating material, CaP has been widely applied to metallic implants. HA-coated implants produce rapid healing responses [6], promote faster bone attachment [7,8], and show a high clinical survival rate [9] when compared to noncoated implants. Furthermore, excellent clinical results were reported for CaP-coated implants when

Received: Jul. 9, 2013; **Accepted:** Oct. 9, 2013

***Correspondence:** Seong-Ho Choi

Department of Periodontology, Research Institute for Periodontal Regeneration, Yonsei University College of Dentistry, 50 Yonsei-ro, Seodaemun-gu, Seoul 120-752, Korea

E-mail: shchoi726@yuhs.ac, Tel: +82-2-2228-3189, Fax: +82-2-392-0398

[†]Ji-Wan Hwang and Eun-Ung Lee contributed equally to this study.

implanted in fresh extraction sites, grafted maxillary sinuses, and type IV bone [10].

However, some reports have suggested that CaP coating may undergo extensive dissolution in tissue fluids and demonstrate rapid breakdown around the implant surface [11,12]. Various chemical compositions of CaP, or coating methods that induce structural changes in the coating, could be the cause of such failure. Among the various coating methods, the plasma spraying technique has been the primary method used to apply CaP coating onto metallic implants. However, this method has demonstrated some problems because of the relatively thick and porous coating it produces [13,14]. Long-term clinical failure has also been reported due to non-uniformity of the coating and low adhesion strength between the metal and the CaP coating [15].

In order to overcome the disadvantages of CaP plasma spray coating, the ion-beam-assisted deposition (IBAD) method has recently been developed. With this method, the dissolution rate of the CaP coating has decreased remarkably while the bonding strength between the layer and Ti substrate has increased [16]. Liu et al. [17] suggested that an atomic intermixing layer is formed between the HA coating and Ti substrate during the IBAD method and this chemical bonding may enhance the interfacial adhesive bonding strength. Furthermore, Lee et al. [18] studied the bone healing of machined implants that were HA coated by the IBAD method in normal bone of rabbit tibiae. Implants coated with CaP by the IBAD method showed a higher bone-to-implant contact ratio compared to those of blasted surface implants and machined surface implants. Kim et al. [19] also demonstrated that implants coated with HA by the IBAD method are biocompatible and show better contact osteogenesis in normal bone. Bone regeneration in clinically challenging bony defects such as gap defects or large dehiscence defects can be different from the healing observed in bones without defects. Several previous studies have shown CaP coating using the IBAD method may improve the bone response and produce a beneficial effect in resolving bony defects [20-22].

During implant surgery, clinicians frequently encounter situations in which it is difficult to obtain mechanical engagement. In particular, poor bone quality and a widened drilling socket may be responsible for rotationally loosened implants. Implant stability is considered to play an important role in successful osseointegration [23]. However, the amount of mechanical engagement required around the implant is yet to be determined. Previous animal studies have revealed favorable outcomes even when the mechanical engagement was not obtained at placement of the implants [24,25]. Furthermore, Jung et al. [24] assumed that osseointegration would be obtained differently according to the absence or

presence of mechanical engagement. In brief, it could be assumed that the newly formed bone in the loosened implant group is composed completely from the bone adjacent to implant surface.

There have been several studies demonstrating the dissolution behavior of the CaP film layer [16,26,27]. Since dissolution behavior is related to bioactivity, it is regarded as an important factor for osseointegration. In a previous study, the Ca/P ratio of the film had a major impact on the dissolution rate, and the dissolution rate decreased in a physiological saline solution with ion-beam assistance [16,18,26,28]. However, the previous studies were based on using mediums such as isotonic saline solution or deionized water, not vital body fluid.

In this study, machined surface implants CaP coated by the IBAD method (CPMS) were placed with one of two different drilling procedures in dogs for 1, 2, or 4 weeks. The aims of this study were (1) to analyze the dissolution behavior of residual CaP particles of removed implants and (2) to evaluate the bone apposition of the CPMS implants in the early healing phase.

MATERIALS AND METHODS

Animals

Five male mongrel dogs (18–24 months; mean body weight, 20–25 kg) were chosen for this study. The animals had intact full dentition and a healthy periodontium. The animal selection, management, surgical protocol, and preparation were carried out according to the routine procedures approved by the Institutional Animal Care and Use Committee, Yonsei Medical Center, Seoul, Korea (certification #2011-0072).

Sample preparation

Cylindrical machined surface implants of commercially pure Ti (3.4 mm in diameter, 10 mm in length) were created (Dentium, Seoul, Korea). The implant surfaces were treated by nanocoating them with CaP at a thickness of 500 nm according to previously published methods [27]. In brief, the evaporants of CaP were prepared by adding 37% CaO powder (Cerac, Milwaukee, WI, USA) to HA powder (Alfa, Ward Hill, MA, USA). The Ca/P ratios of the evaporants were higher than 1.67. For the CaP coating, an electron beam evaporator (Telemark, Fremont, CA, USA) and an end-Hall-type ion gun (Mark II, Commonwealth Scientific, Alexandria, VA, USA) were employed. Once a suitable vacuum was attained, an ion beam was introduced into the vacuum chamber and the evaporants adhered to the surface of the implants. Heat treatment after the CaP coating was conducted at 450°C in a vacuum of 0.003 mmHg for 1 hour.

Experimental design

CaP dissolution behavior analysis

The implant beds were prepared and a total of 8 CPMS implants were bilaterally placed in the mandible of two dogs. Groups were divided according to the healing periods (0, 1, 2, and 4 weeks) and existence of initial stability (nonmobile implant [NI] and rotational implant [RI]).

Bone apposition analysis ($n=2$)

A total of 12 CPMS implants were bilaterally placed in the mandible of three dogs. The groups were divided according to healing periods (1, 2, and 4 weeks) and the existence of initial stability (NI and RI). Two implants per group were placed.

Surgical protocol

The entire surgical procedures were performed under general and infiltration anesthesia in a sterile operating room. The animals received a preanesthetic intravascular injection of atropine (0.05 mg/kg; Kwangmyung Pharmaceutical Co., Seoul, Korea) and an intramuscular injection of xylazine (2 mg/kg; Rompun, Bayer Korea, Seoul, Korea) and ketamine hydrochloride (10 mg/kg; Ketalar, Yuhan, Seoul, Korea). Two percent enflurane (Gerolan, Choongwae Pharmaceutical Co., Seoul, Korea) was administered as inhalation anesthesia. After disinfection of the surgical site, infiltration anesthesia was administered using lidocaine (2% lidocaine hydrochloride-epinephrine 1:100,000; Kwangmyung Pharmaceutical Co.). The animals were monitored with an electrocardiogram. Crevicular incisions were made, and all of the premolars (P1–P4) were carefully extracted. The flaps were sutured with 4-0 Monosyn (Glyconate absorbable monofilament, B-Braun, Aesculap Inc., Center Valley, PA, USA).

For bone deposition analysis, the implants were placed after an 8-week healing period using the same surgical conditions as those for tooth extraction. A midcrestal incision and full-thickness mucoperiosteal flap was made bilaterally and implant ostectomy was performed. The final drill used in the NI groups was 2.85 mm in diameter according to the standard drilling protocol. The 3.3-mm diameter drill was last used prior to implant installation in the RI groups according to the oversized drilling protocol. The countersink drill was used to avoid a potential effect on primary stability of the cortical bone. Once the implant site was prepared, the implants of the same fixture size (3.4-mm diameter, 10-mm length) were inserted (Fig. 1). In the RI groups, the vertical and rotational mobility was confirmed, and the fixture adaptor was gently removed after the insertion of the fixture. The incision was closed with 4-0 Monosyn (B-Braun, Aesculap Inc.), leaving the implants submerged during the healing period. The dogs were fed a soft diet for 2 weeks, and the sutures were removed

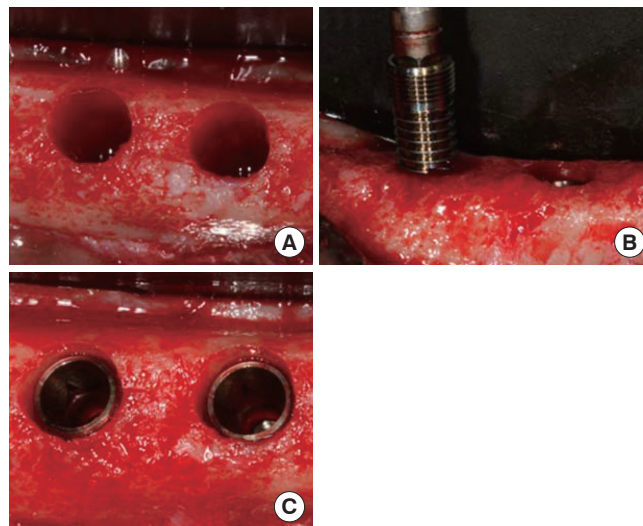


Figure 1. Clinical photographs of the experiment. (A) Implant sites were prepared, (B) calcium phosphate-coated machined surface implants were inserted, and (C) after implant placement.

after 10 days. Two NI implants and two RI implants were placed bilaterally in three male mongrel dogs, and a dog was sacrificed at each of 1, 2, and 4 weeks after surgery.

For CaP dissolution behavior analysis, eight implants were placed in two male mongrel dogs. Two implants (0-NI and 0-RI) were removed immediately after insertion. The other six implants were removed after 1-, 2-, and 4-week healing periods. All of the implants were removed by hand ratchet, then the removed implants were washed in distilled water in order to eliminate blood from the implant surface.

CaP dissolution behavior analysis

The surface morphology of the unused implant before insertion and the removed implants was observed by scanning electron microscopy (SEM, S-4200, Hitachi, Tokyo, Japan) operating at 15.0 kV. The SEM studies were coupled with energy dispersive spectrometer (EDS) equipment to investigate the calcium and phosphorus deposition of the coatings.

Bone apposition analysis

Clinical observation

The animals were carefully observed for inflammation, exposure of implants, and other complications during the post-operative healing period until the time of sacrifice.

Histologic and histometric analysis

The block sections were fixed in 10% neutral buffered formalin for 10 days. They were then dehydrated in ethanol, embedded in methacrylate, and sectioned in the buccolingual plane. The central section from each specimen was re-

duced to a final thickness of about 20 μm by microgrinding (Exakt, Norderstedt, Germany). The sections were stained with hematoxylin-eosin. A general histological analysis was performed using polarized light microscopy (Research System Microscope BX51, Olympus Co., Tokyo, Japan). After microscopic examination, histometric measurements were performed by one blinded investigator using a PC-based automated image analysis (Image-Pro Plus; Media Cybernetics, Silver Spring, MD, USA). The measurement parameters were as follows:

- (1) Bone-to-implant contact (BIC%) in the six most coronal threads of the implant was defined as the proportion of the linear length of the bone in contact with the implant over the total length of the implant surface.
- (2) Bone density (BD%) within the six most coronal threads of the implant was defined as the proportion of the bone areas over the total areas between the imaginary line connecting the top of the thread and the fixture lines.

The parameters are presented as a mean value with a standard deviation ($n=2$). Statistical analysis was not performed due to the small sample size.

RESULTS

CaP dissolution behavior analysis

Surface morphology

Fig. 2 shows SEM micrographs of the unused CPMS implant and two of the removed implants (o-NI, 2-NI). The surface of the unused CPMS implant presented a surface with microroughness and parallel grooves, which is the typical

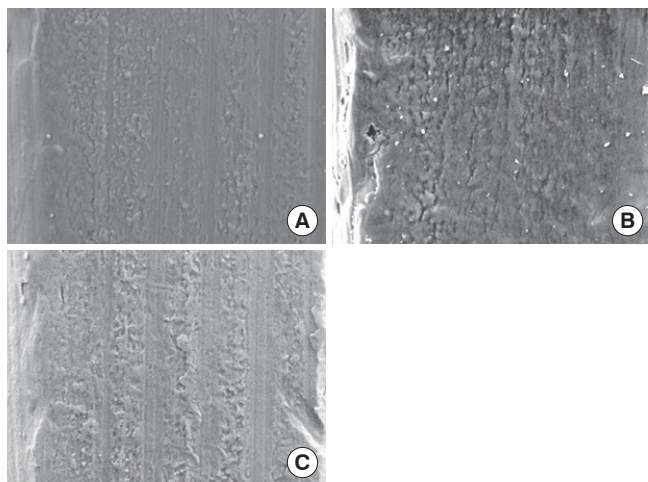


Figure 2. Scanning electron microscopy analysis of implant surfaces ($\times 1,000$). (A) Unused implant before insertion, (B) nonmobile implant (NI) that was removed immediately after insertion (o-NI), and (C) nonmobile implant that was removed after a 2-week healing period (2-NI).

outcome of the grinding process. The surfaces of the implant that was removed immediately after insertion (o-NI) and the implant that was removed after a 2-week healing period (2-NI) also had a microrough surface with parallel grooves along the polishing direction. All of the implants had little bone tissue attached to the surface. There were no significant differences among the surfaces of the implants.

Surface composition

Figs. 3 and 4 are examples of EDS data showing peaks corresponding to the different elements present in the eight implant surfaces that were retrieved and analyzed. EDS analysis exhibited the presence of calcium and phosphorus elements on the surfaces of the two implants that had been removed immediately after insertion (o-NI and o-RI). There were peaks corresponding to calcium and phosphorus in addition to Ti and oxygen. However, the other six implants were composed mainly of Ti. Only small percentages of calcium and phosphorus were detected in two implants (2-NI and 4-RI).

Bone apposition analysis

Clinical findings

Wound healing was uneventful during the postoperative healing period, with no complications (i.e., severe swelling, bleeding, allergic reactions, inflammatory reactions, or exposure of implants) found in any of the groups.

Histologic results

In the NI group, a triangular thread tip was partly engaged with the native bone and an osteotomy line demarcating the drilled margin was clearly present at 1 week and 2 weeks of healing (Fig. 5A and B). At 1 week of healing, most portions of the wound chambers were occupied by connective tissue that was rich in vascular structures. A few bone particles were found in provisional soft tissue (Fig. 5A). At 2 weeks of healing, woven bone formation was pronounced and portions of woven bone extended from the native bone into the connective bone. Projection of newly formed woven bone had reached the surface of the implant in some areas (Fig. 5B). At 4 weeks, the osteotomy line was less clear. The newly formed mineralized bone extended from the native bone into the wound chamber and most portions of the implant surface were covered with woven bone (Fig. 5C).

There were no notable differences between the NI and RI groups in the healing process. In the RI group, an osteotomy line was seen away from the implant thread tip in the 1-week and 2-week healing groups (Fig. 6A and B). The amount of newly formed bone increased with healing time. At 4 weeks of healing, osteotomy lines were not observed at the bone-

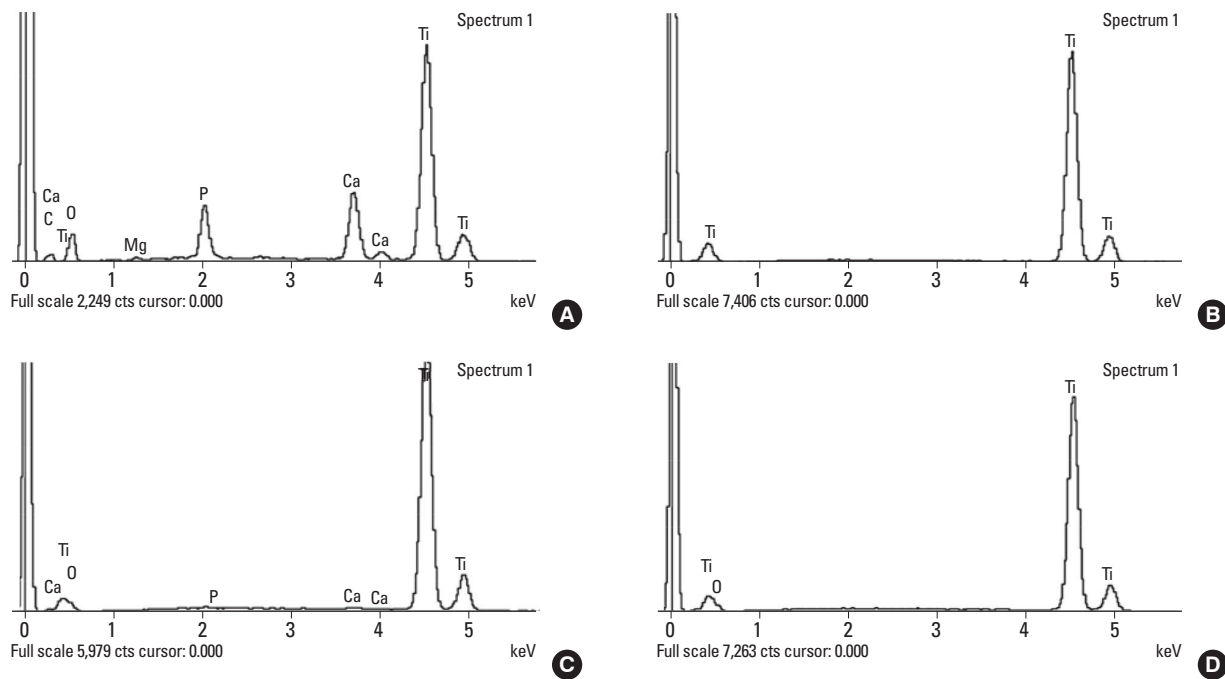


Figure 3. Energy dispersive spectrometer analysis of surface of nonmobile implant (NI) group. (A) Implant that was removed immediately after insertion (o-NI), (B) implant that was removed after a 1-week healing period (1-NI), (C) implant that was removed after a 2-week healing period (2-NI), and (D) implant that was removed after a 4-week healing period (4-NI). Ti: titanium, Ca: calcium, P: phosphorus, O: oxygen, Mg: magnesium, C: carbon, Ti: titanium.

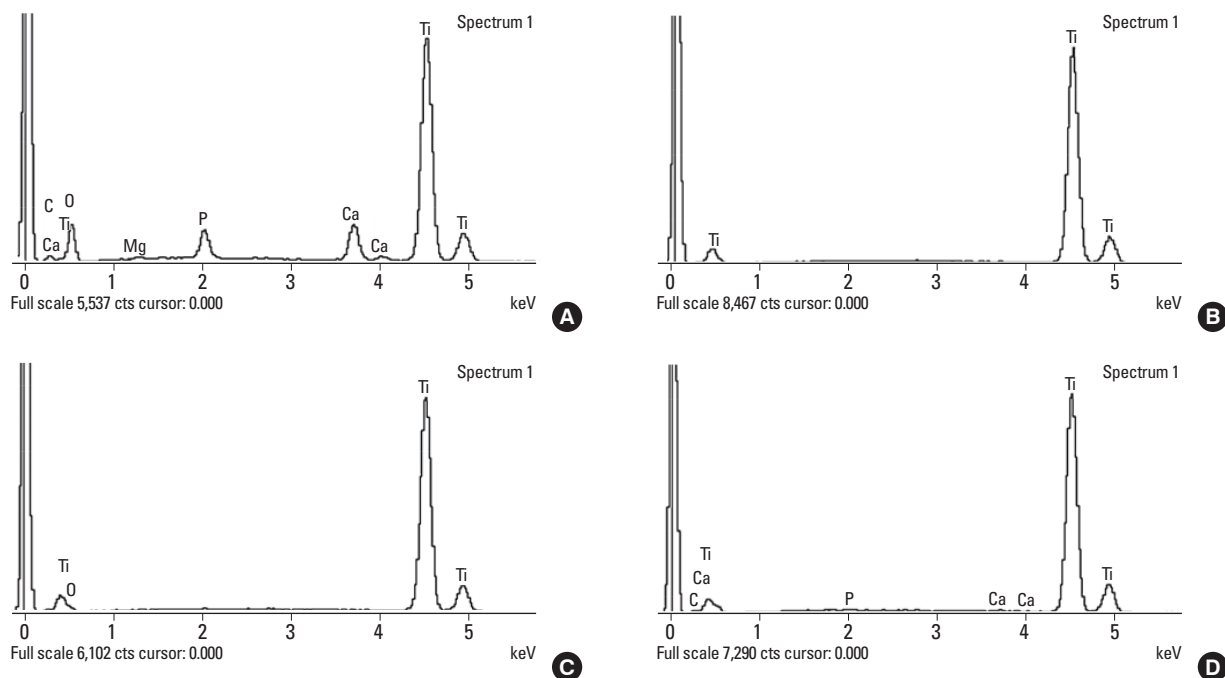


Figure 4. Energy dispersive spectrometer analysis of the surface of the rotational implant (RI) group. (A) Implant removed immediately after insertion (o-RI), (B) implant removed after a 1-week healing period (1-RI), (C) implant removed after a 2-week healing period (2-RI), and (D) implant removed after a 4-week healing period (4-RI). Ti: titanium, Ca: calcium, P: phosphorus, O: oxygen, Mg: magnesium, C: carbon, Ti: titanium.

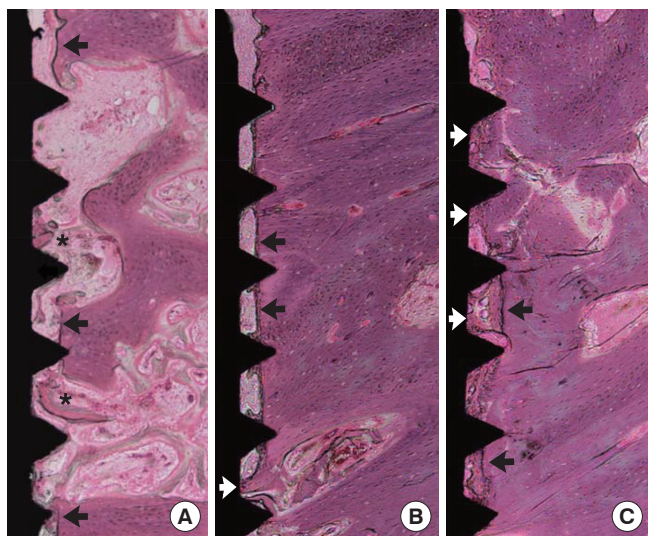


Figure 5. Representative photomicrographs of the nonmobile implant group (H&E, $\times 50$). (A) At 1 week of healing, (B) at 2 weeks of healing, and (C) at 4 weeks of healing. Black arrow: osteotomy line; White arrow: where newly formed woven bone had reached the implant surface; Asterisk: bone particle.

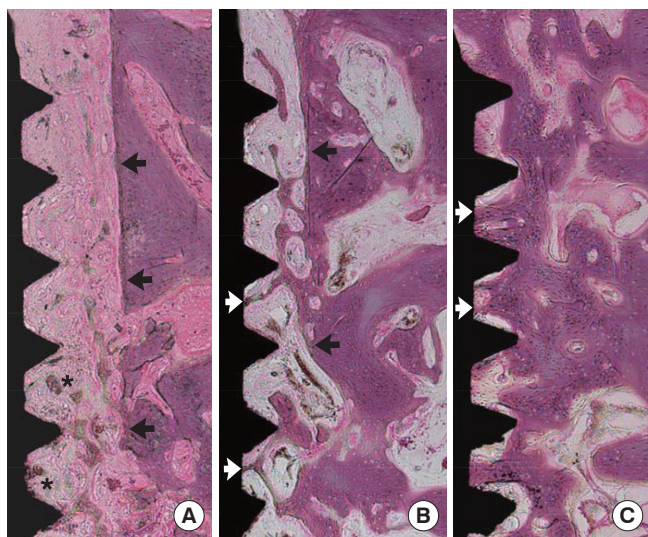


Figure 6. Representative photomicrographs of the rotational implant group (H&E, $\times 50$). (A) At 1 week of healing, (B) at 2 weeks of healing, and (C) at 4 weeks of healing. Black arrow: osteotomy line; White arrow: where newly formed woven bone had reached the implant surface; Asterisk: bone particle.

implant interface, and the density of the newly formed bone was comparable to that of the existing bone (Fig. 6C).

At 4 weeks in both groups, bone formation occurred predominantly on the exposed bone surfaces along the microthread area at the coronal part of the implants (Fig. 7A). On the other hand, a narrow rim of new bone was apparently apposed along the apical part of the implants (Fig. 7B).

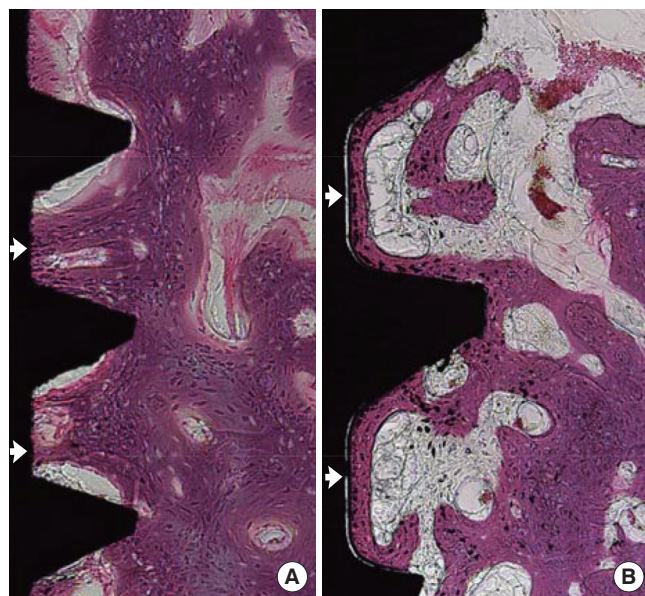


Figure 7. Representative photomicrographs from two different bone appositional perspectives from a rotational implant specimen at 4 weeks of healing (H&E, $\times 100$). (A) Distant osteogenesis was observed on the coronal part of the implant surface. (B) Contact osteogenesis was observed on the apical part of the implant surface. White arrow: newly formed bone.

Table 1. Mean of bone-to-implant contact percentages after implant placement and removal (n=2).

Time of removal and analysis	Nonmobile Implant	Rotational Implant
1 week	19.66 \pm 15.81	0 \pm 0
2 weeks	43.06 \pm 8.49	7.19 \pm 1.68
4 weeks	59.32 \pm 8.27	50.01 \pm 2.77

Values are presented as mean \pm standard deviation.

Table 2. Mean of bone density percentages and implant placement and removal (n=2).

Time of removal and analysis	Nonmobile Implant	Rotational Implant
1 week	22.80 \pm 7.49	0 \pm 0
2 weeks	50.97 \pm 9.60	16.57 \pm 8.63
4 weeks	68.29 \pm 7.89	63.53 \pm 4.01

Histometric results

The histometric analysis of the 12 implants (n=2) is presented in Tables 1 and 2. The BIC and BD parameters are in accordance with the histological findings. The mean values of the BIC and BD in the NI implant group increased gradually with healing time. The mean values of the BIC and BD were lower in the RI group than those of the NI group in all healing periods. However, the BIC and BD in the RI groups showed a remarkable increase after 2 weeks of healing and were comparable to those of the NI group at 4 weeks of healing.

DISCUSSION

In the present study, we assessed the dissolution behavior and early bone apposition of CaP-coated machined surface implants. There is an effort to improve the surface of implants in order to enhance the quality and quantity of osseointegration. The surface modification of implants includes chemical and mechanical treatment. By increasing the level of roughness mechanically, rough-surfaced implants showed an increased survival rate and BIC. Lang et al. [29] concluded that moderately rough surfaces showed the highest level of BIC and provided enhanced bone integration compared with smooth and minimally rough surfaces in a consensus report. In spite of the advantages of rough-surfaced implants in the early healing phase, rough-surfaced implants are more likely to develop peri-implantitis than minimally rough implants and machined surfaces once exposed to the oral environment [30]. The results could be caused by the composition and amount of biofilm formation that were influenced by surface characteristics. Thus, a machined surface contributes to controlling bacterial accumulation during the maintenance period.

Among various CaP coating methods, CaP coating by the IBAD method has been widely investigated recently because of the improved biocompatibility and excellent bonding strength it enables [16-18]. Lee et al. [18] demonstrated that the mean value of the BIC was 52.4% for the CaP coating on machined implants, which was higher than 48.5% for the blasted ones in a rabbit model. In addition, a previous study showed that CaP-nanocoated machined surface implants had a comparable BIC to CaP-nanocoated roughened surface implants in a dog model [31]. However, these previous studies evaluated the late bone response after a 12-week healing period. Here, the early bone response was analyzed at 1, 2, and 4 weeks postsurgery using two different drilling protocols.

Fig. 2 shows SEM micrographs of the surfaces of implants. The unused implant before insertion showed microroughness with a typical smooth surface texture (Fig. 2A). There were no significant differences between the unused implants and removed implants (Fig. 2B and C). The finding that there was no bone tissue attached to the removed implant surfaces could be explained by the surface properties of CPMS implants. Machined surface implants have little mechanical bone interlocking effect, unlike roughened surface implants. In previous studies, CPMS implants increased the removal torque force more than 50% compared to machined implants without CaP, and they required a slightly higher removal torque force than did the blasted implants [27]. From these observations, we can verify that chemical bonding of bone to CPMS implants enhanced bone apposition despite not hav-

ing a mechanical bone interlocking effect.

In EDS analysis, calcium and phosphorus were detected in two implants that were removed immediately after insertion (Figs. 3A and 4A). There were no notable differences between o-NI and o-RI. Because the NI group was installed and removed with a 'press fit' method via mechanical compression, it may be assumed that the CaP coating film of the implant surface was not removed by friction during implant placement and removal. This result is consistent with the results of previous studies on bonding strength. The tensile bonding strength of HA coating by the IBAD method was 70 ± 2 MPa [32], whereas that of HA coating by the plasma spraying method has been reported to be 31.9 MPa [33].

However, six implants were composed mainly of Ti and only small percentages of calcium and phosphorus were detected in two implants (2-NI and 4-RI). The results may have been affected by the potential detachment of the CaP coating layer as a result of mechanical friction during fixture removal and the binding forces between the CaP layer and the surrounding tissues, contributing to a limitation of this experiment. The dissolution rate of the coating layer is affected by the Ca/P ratio and surface crystallinity. CaP coating by the IBAD method produces a coating layer with a low dissolution rate in physiological saline solution by increasing the Ca/P ratio [16]. Film with a Ca/P ratio of 1.5 dissolved in 48 hours, whereas a plasma-sprayed HA coating dissolved completely within 8 hours [28]. When CaP film with a Ca/P ratio of 1.62 was coated on implants, the average dissolution rate in a saline solution was 47.5 nm/hr [18]. In the present study, in which the experiment was performed in vital body fluid, the CaP coating dissolved almost completely within 1 week. It could be inferred that the CaP thin film dissolved in the early healing phase and biomimetic apatite was formed at the implant surface, similarly to the results of a previous study [26]. Furthermore, the dissolution rate was not affected by the situation in which the bone was not directly in contact with its surface from the results of the RI group.

The present study included two types of experimental models: nonmobile and rotational implants. These mimicked the clinical situations in which the implants were installed with recommended fixation torque (20–40 N) and limited fixation. In histologic analysis, woven bone formation was pronounced at 2 weeks' healing and most portions of the implant surface were covered with woven bone in both groups (NI and RI). At 4 weeks' healing, the osteotomy line was less clear and there were no notable differences between the groups. This means that the CPMS implants were successfully osseointegrated in the early healing period regardless of the different drilling procedures. These results are consistent with the results of a previous study using sand-

blasted, large grit, acid-etched surfaced implants [24]. Two types of peri-implant bone regeneration have been identified in the literature [6,34]. Distance osteogenesis occurs when new bone formation is initiated at the surrounding old bone surface. On the other hand, contact osteogenesis occurs when osteogenic cells migrate to the implant surface and begin laying down new bone directly onto the implant. Histological observation revealed that bone apposition occurred predominantly from the adjacent existing bone tissue (distant osteogenesis) along the microthread area at the coronal part of the implants in both the NI and RI groups. The result can be explained by vascular disruption of the cortical bone. During implant site preparation, vascular disruption of the cortex leads to death of the peri-implant cortical bone and slow remodeling by osteoclast invasion from the underlying medullary compartment occurs [6]. Contact osteogenesis was also observed along the apical medullary part of the implant surface in both the NI and RI groups.

In the histometric analysis, only the coronal microthread area was evaluated due to the invasion of the inferior alveolar nerve in the apical region. The BD and BIC values of the RI group increased remarkably after 2 weeks' healing and were comparable to those of the NI group at 4 weeks' healing. Thus, the CPMS implants showed a rapid ability to achieve bone apposition in comparison to previous results with machined implants without CaP coatings at 4 weeks of healing [19,35], even if the mechanical engagement was not obtained.

CaP-nanocoated implant surfaces are considered to have a strong interaction between the implant and surrounding bone by chemical bonding, while highly roughened surfaces such as grit-blasted or Ti plasma-sprayed implants have been shown to favor mechanical anchorage and fixation to bone [36]. When calcium and phosphorus ions dissolved and reprecipitated, the chemical interaction between CaP and Ca²⁺ binding protein modified the composition and structure of the coating surface [37]. As a result, the surface chemical properties of the electrochemically calcium-incorporated Ti oxide led to reinforced osseointegration [38]. The present study demonstrated early dissolution behavior within 1 week and enhanced bone apposition of CPMS implants in the early healing phase. From these results, an early loading protocol with CPMS implants can be performed clinically.

However, there are a few limitations to the present study. Because the sample size was too small to perform statistical analysis, further studies on the correlation between the dissolution rate and bone formation with a larger sample size should be conducted.

In conclusion, within the limits of this study, it can be speculated that CaP coating of CPMS implants dissolves in the early healing phase and induces early bone formation chem-

ically, regardless of mechanical engagement.

CONFLICT OF INTEREST

No potential conflict of interest relevant to this article was reported.

ACKNOWLEDGEMENTS

This work was supported by a grant (code #: 2011K000191) from the Center for Nanostructured Materials Technology under the 21st Century Frontier R&D Program of the Ministry of Education, Science and Technology; and was supported by the Basic Science Research Program through the National Research Foundation of Korea (NRF) funded by the Ministry of Education, Science and Technology, Republic of Korea (#2012051022).

REFERENCES

1. Tjellstrom A, Lindstrom J, Hallen O, Albrektsson T, Brånemark PI. Osseointegrated titanium implants in the temporal bone: a clinical study on bone-anchored hearing aids. *Am J Otol* 1981;2:304-10.
2. Cooper LF. A role for surface topography in creating and maintaining bone at titanium endosseous implants. *J Prosthet Dent* 2000;84:522-34.
3. Shalabi MM, Gortemaker A, Van't Hof MA, Jansen JA, Creugers NH. Implant surface roughness and bone healing: a systematic review. *J Dent Res* 2006;85:496-500.
4. Wennerberg A, Albrektsson T. Effects of titanium surface topography on bone integration: a systematic review. *Clin Oral Implants Res* 2009;20 Suppl 4:172-84.
5. Han T, Carranza FA Jr, Kenney EB. Calcium phosphate ceramics in dentistry: a review of the literature. *J West Soc Periodontol Periodontol Abstr* 1984;32:88-108.
6. Davies JE. Understanding peri-implant endosseous healing. *J Dent Educ* 2003;67:932-49.
7. Morimoto K, Kihara A, Takeshita F, Akedo H, Suetsugu T. Differences between the bony interfaces of titanium and hydroxyapatite-alumina plasma-sprayed titanium blade implants. *J Oral Implantol* 1988;14:314-24.
8. Kay JF. Calcium phosphate coatings for dental implants. Current status and future potential. *Dent Clin North Am* 1992;36:1-18.
9. McGlumphy EA, Peterson LJ, Larsen PE, Jeffcoat MK. Prospective study of 429 hydroxyapatite-coated cylindrical omniloc implants placed in 121 patients. *Int J Oral Maxillofac Implants* 2003;18:82-92.
10. Biesbrock AR, Edgerton M. Evaluation of the clinical pre-

- dictability of hydroxyapatite-coated endosseous dental implants: a review of the literature. *Int J Oral Maxillofac Implants* 1995;10:712-20.
11. Liao H, Fartash B, Li J. Stability of hydroxyapatite-coatings on titanium oral implants (IMZ): 2 retrieved cases. *Clin Oral Implants Res* 1997;8:68-72.
 12. Hanisch O, Cortella CA, Boskovic MM, James RA, Slots J, Wikesjo UM. Experimental peri-implant tissue breakdown around hydroxyapatite-coated implants. *J Periodontol* 1997;68:59-66.
 13. Klein CP, Patka P, van der Lubbe HB, Wolke JG, de Groot K. Plasma-sprayed coatings of tetracalciumphosphate, hydroxyl-apatite, and alpha-TCP on titanium alloy: an interface study. *J Biomed Mater Res* 1991;25:53-65.
 14. Hayashi K, Inadome T, Mashima T, Sugioka Y. Comparison of bone-implant interface shear strength of solid hydroxyapatite and hydroxyapatite-coated titanium implants. *J Biomed Mater Res* 1993;27:557-63.
 15. Albrektsson T. Hydroxyapatite-coated implants: a case against their use. *J Oral Maxillofac Surg* 1998;56:1312-26.
 16. Choi JM, Kim HE, Lee IS. Ion-beam-assisted deposition (IBAD) of hydroxyapatite coating layer on Ti-based metal substrate. *Biomaterials* 2000;21:469-73.
 17. Liu JQ, Luo ZS, Cui FZ, Duan XF, Peng LM. High-resolution transmission electron microscopy investigations of a highly adhesive hydroxyapatite coating/titanium interface fabricated by ion-beam-assisted deposition. *J Biomed Mater Res* 2000;52:115-8.
 18. Lee IS, Kim DH, Kim HE, Jung YC, Han CH. Biological performance of calcium phosphate films formed on commercially pure Ti by electron-beam evaporation. *Biomaterials* 2002;23:609-15.
 19. Kim MK, Choi JY, Chae GJ, Jung UW, Kim ST, Lee IS, et al. The histometric analysis of osseointegration in hydroxyapatite surface dental implants by ion beam-assisted deposition. *J Korean Acad Periodontol* 2008;38(Suppl):363-72.
 20. Yoon HJ, Song JE, Um YJ, Chae GJ, Chung SM, Lee IS, et al. Effects of calcium phosphate coating to SLA surface implants by the ion-beam-assisted deposition method on self-contained coronal defect healing in dogs. *Biomed Mater* 2009;4:044107.
 21. Chae GJ, Jung UW, Jung SM, Lee IS, Cho KS, Kim CK, et al. Healing of surgically created circumferential gap around Nano-coating surface dental implants in dogs. *Surf Interface Anal* 2008;40:184-7.
 22. Um YJ, Song JE, Chae GJ, Jung UW, Chung SM, Lee IS, et al. The effect of post heat treatment of hydroxyapatite-coated implants on the healing of circumferential coronal defects in dogs. *Thin Solid Film* 2009;517:5375-9.
 23. Meredith N. Assessment of implant stability as a prognostic determinant. *Int J Prosthodont* 1998;11:491-501.
 24. Jung UW, Kim S, Kim YH, Cha JK, Lee IS, Choi SH. Osseointegration of dental implants installed without mechanical engagement: a histometric analysis in dogs. *Clin Oral Implants Res* 2012;23:1297-301.
 25. Blanco J, Alvarez E, Munoz F, Linares A, Cantalapiedra A. Influence on early osseointegration of dental implants installed with two different drilling protocols: a histomorphometric study in rabbit. *Clin Oral Implants Res* 2011;22:92-9.
 26. Kim H, Choi SH, Chung SM, Li LH, Lee IS. Enhanced bone forming ability of SLA-treated Ti coated with a calcium phosphate thin film formed by e-beam evaporation. *Biomed Mater* 2010;5:044106.
 27. Lee IS, Zhao BH, Lee GH, Choi SH, Chung SM. Industrial application of ion beam assisted deposition on medical implants. *Surf Coat Technol* 2007;201:5132-7.
 28. Lee IS, Kim HE, Kim SY. Studies on calcium phosphate coatings. *Surf Coat Technol* 2000;131:181-6.
 29. Lang NP, Jepsen S; Working Group 4. Implant surfaces and design (Working Group 4). *Clin Oral Implants Res* 2009;20 Suppl 4:228-31.
 30. Lang NP, Berglundh T; Working Group 4 of Seventh European Workshop on Periodontology. Periimplant diseases: where are we now? Consensus of the Seventh European Workshop on Periodontology. *J Clin Periodontol* 2011;38 Suppl 11:178-81.
 31. Choi JY, Jung UW, Kim CS, Jung SM, Lee IS, Choi SH. Influence of nanocoated calcium phosphate on two different types of implant surfaces in different bone environment: an animal study. *Clin Oral Implants Res* 2013;24:1018-22.
 32. Cui FZ, Luo ZS, Feng QL. Highly adhesive hydroxyapatite coatings on titanium alloy formed by ion beam assisted deposition. *J Mater Sci Mater Med* 1997;8:403-5.
 33. Zablotsky M, Meffert R, Mills O, Burgess A, Lancaster D. The macroscopic, microscopic and spectrometric effects of various chemotherapeutic agents on the plasma-sprayed hydroxyapatite-coated implant surface. *Clin Oral Implants Res* 1992;3:189-98.
 34. Davies JE. Mechanisms of endosseous integration. *Int J Prosthodont* 1998;11:391-401.
 35. Abrahamsson I, Berglundh T, Linder E, Lang NP, Lindhe J. Early bone formation adjacent to rough and turned endosseous implant surfaces: an experimental study in the dog. *Clin Oral Implants Res* 2004;15:381-92.
 36. Novaes AB Jr, de Souza SL, de Barros RR, Pereira KK, Iezzi G, Piattelli A. Influence of implant surfaces on osseointegration. *Braz Dent J* 2010;21:471-81.
 37. Feng B, Chen J, Zhang X. Interaction of calcium and phos-

- phate in apatite coating on titanium with serum albumin. *Biomaterials* 2002;23:2499-507.
38. Sul YT, Johansson CB, Albrektsson T. Oxidized titanium screws coated with calcium ions and their performance in rabbit bone. *Int J Oral Maxillofac Implants* 2002;17:625-34.